Chapter 9
Formation of K–Cr Titanates from Reactions of Chromite and Ilmenite/Rutile with Potassic Aqueous-Carbonic Fluid: Experiment at 5 GPa and Applications to the Mantle Metasomatism

V. G. Butvina, S. S. Vorobey, O. G. Safonov, and G. V. Bondarenko

Abstract Magnetoplumbite (yimengite-hawthorneite, HAWYIM), crichtonite (lindsleyite-mathiasite, LIMA) and hollandite (priderite) minerals are exotic titanate phases, which formed during metasomatism at the conditions of high alkali activity, especially K, in the fluids in the upper mantle peridotites. The paper presents data on experiments on formation of K-end-members priderite, yimengite and mathiasite, as the result of the interaction of chromite, chromite + rutile and chromite + ilmenite assemblages in the presence of a small amount of silicate material with H_2O–CO_2–K_2CO_3 fluids at 5 GPa and 1200 °C. Cr-bearing Ba-free priderite, characteristic for metasomatized Cr-rich harzburgites, was firstly synthesized. The experiments demonstrated the principal possibility of the formation of the titanates in the reactions of chromite with alkaline aqueous-carbonic fluids and melts. However, the formation of these phases does not proceed directly on chromite, but requires additional titanium source. The relationship between titanates is found to be a function of the activity of the potassium component in the fluid/melt. Priderite is an indicator of the highest potassium activity in the mineral-forming medium. Titanates in the run products are constantly associated with phlogopite. Experiments prove that the formation of titanates manifests the most advanced or repeated stages of metasomatism in mantle peridotites. Association of titanates with phlogopite characterizes a higher activity of the potassium component in the fluid/melt than the formation of phlogopite alone. The examples from natural associations, reviewed in the paper, well illustrate these conclusions.

V. G. Butvina (✉) · O. G. Safonov · G. V. Bondarenko
D.S. Korzhinskii Institute of Experimental Mineralogy, Russian Academy Sciences, Academician Ossipian str. 4, Chernogolovka, Moscow Region, Russia 142432
e-mail: butvina@iem.ac.ru

S. S. Vorobey · O. G. Safonov
Geological Department, Lomonosov Moscow State University, Vorob'evy Gory, Moscow, Russia 119899

Y. Litvin and O. Safonov (eds.), *Advances in Experimental and Genetic Mineralogy*, Springer Mineralogy, https://doi.org/10.1007/978-3-030-42859-4_9

Keywords K-Cr titanates · Yimengite · Priderite · Mathiasite · Potassic fluid · Peridotite · Mantle metasomatism · High pressure experiment

9.1 Introduction

The term "mantle metasomatism" (Lloyd and Bailey 1975; Harte and Gurney 1975; Bailey 1982, 1987; Menzies and Hawkesworth 1987) combines the processes of transformation of mantle rocks under the influence of external fluids and/or melts, regardless of their origin and composition. The metasomatic processes in the upper mantle are responsible not only for great variability of parageneses in the mantle rocks, but also for formation of magmas specific in composition, such as kimberlites, carbonatites, lamproites, kamafugites and others (e.g., Haggerty 1987). The type of mantle metasomatism, expressed in the formation of new phases, which are non-characteristic of the peridotites and eclogites, Harte (1983) referred to as the "modal mantle metasomatism". This process is commonly expressed in the formation of amphiboles, phlogopite, apatite, carbonates, sulfides, titanite, ilmenite, rutile. A number of unique mineral phases form as the products of metasomatism in the mantle. Among them are minerals of magnetoplumbite (yimengite-hawthorneite, HAWYIM), crichtonite (lindsleyite-mathiasite, LIMA) and hollandite (priderite) groups (Haggerty 1991), i.e. rare K–Ba titanates, enriched in large-ion lithophile (LILE), high field strength (HFSE), light rare earth (LREE) elements, U and Th.

Yimengite K (Cr, Ti, Mg, Fe, Al)$_{12}$O$_{19}$ is the end-member of the magnetoplumbite group with general formula AM$_{12}$O$_{19}$ (Haggerty 1991). The 12-coordinated site A in the structure of this mineral is located in perovskite-like layers (AMO$_3$) and contains large cations (K, Ba and LILE), while small cations M (Ti, Cr, Fe, Mg, Zr, Nb, V, Zn) are located in 4 to- 6-coordinated polyhedra in spinel-like layers (Grey et al. 1987). Yimengite forms a limited solid solution with hawthorneite Ba (Cr, Ti, Mg, Fe, Al)$_{12}$O$_{19}$ (Haggerty et al. 1989). Natural minerals of yimengite-hawthorneite series (HAWYIM) usually do not correspond to an ideal formula, being characterized by significant variations component populations in both sites and vacancies in the structure. Yimengite was first described in kimberlite dykes of the Shandong province, China (Dong et al. 1983) in association with olivine, chromian pyrope, chromite, phlogopite, ilmenite, chromian diopside, apatite, zircon, moissanite. As a product of modifications of chromite xenocrysts, yimengite was identified in the heavy concentrates of the kimberlites of the Guaniamo area, Venezuela (Nixon and Condliffe 1989), and Float-Ouellet, Australia (Kiviets et al. 1998). In all cases, yimengite contains BaO (up to 3.4 wt% in yimengite from Venezuela), indicating a solid solution with hawthorneite (Grey et al. 1987; Haggerty et al. 1989; Peng and Lu 1985). The compositional characteristics of chromite, after which yimengite forms, indicate that they belong to the assemblage of diamondiferous garnet harzburgites (Nixon and Condliffe 1989). Yimengite was discovered as the inclusions in diamonds (Sobolev et al. 1988, 1998; Bulanova et al. 2004), where it is also associated with the typical minerals of harzburgite paragenesis, i.e. chromite, chromian subcalcic garnet and

enstatite. Inclusions of yimegite described by Bulanova et al. (2004) contain elevated Rb, Cs, Sr concentrations. According to some authors, yimengite is a product of reactions of diamond-bearing harzburgites at the base of the lithospheric continental mantle at depths of about 150 km with fluids enriched in K, HFSE, LREE. This is confirmed by the discovery of yimegite and hawthorneite in metasomatic veins, which cross harzburgite xenolith from a kimberlite pipe Bultfontein (South Africa) along with phlogopite, K-richterite, the LIMA phases, armalcolite, rutile, ilmenite (Haggerty et al. 1986).

Mathiasite is titanate of the crichtonite group $AM_{21}O_{38}$, where the position of A is characterized by isomorphism Ba ↔ K (lindsleyite-mathiasite, LIMA). Firstly, lindsleyite and mathiasite were identified by Haggerty (1975) in the De Beers kimberlite pipe, South Africa. Subsequently, the minerals were described in the metasomatized peridotite xenoliths from other kimberlite pipes of South Africa (Erlank and Rickard 1977; Smyth et al. 1978; Jones et al. 1982; Konzett et al. 2000, 2013). In the metasomatized peridotites, it occurs both as end-members of the LIMA series and as intermediate members of the solid solution. Characteristic minerals associated with the LIMA are phlogopite, diopside, K-richterite, Nb–Cr-rutile, Mg–Cr–Nb-ilmenite and Mg–Cr spinel (Haggerty et al. 1983). The LIMA minerals are described as inclusions in xenocrysts of chromian pyrope (Rezvukhin et al. 2018) and in diamonds (Sobolev and Yefimova 2000) from kimberlites.

Priderite is titanate of hollandite group, solid solution in the system of $A^{2+}B^{2+}Ti_7O_{16}$–$A^{+}{}_2B^{2+}Ti_7O_{16}$–$A^{2+}B^{3+}{}_2Ti_6O_{16}$–$A^{+}{}_2B^{3+}{}_2Ti_6O_{16}$. The site A is occupied by Ba and K, as well as Na, Pb, Sr, Ca and REE; the site B holds Mg, Fe^{2+}, Fe^{3+}, Al, Cr, substituting Ti. Priderite was firstly described by Prider (1939) and Norrish (1951) in the Kimberly lamproites, Western Australia, and was subsequently found as a typomorphic mineral of leucite lamproites (Jaques et al. 1989). It is known in metasomatized peridotite xenoliths from kimberlites (Konzett et al. 2013; Giuliani et al. 2012; Naemura et al. 2015; Haggerty 1987), as well as diamond inclusions (Jaques et al. 1989). Chrome-dominant variety of priderite is found in the metasomatized peridotites only (Haggerty 1987, 1991; Konzett et al. 2013; Giuliani et al. 2012; Naemura et al. 2015).

Experimental data on the stability of K–Ba-titanates are limited to several studies. Podpora and Lindsley (1984) synthesized lindsleyite and mathiasite with compositions given by Haggerty et al. (1983) at 2 GPa/1300 °C and 2.2 GPa/900 °C. Foley et al. (1994) studied stability of priderite, its Fe^{3+} and Fe^{2+}-bearing varieties, as well as HAWYIM and LIMA phases in experiments on synthesis from oxide and simple titanate mixtures at 3.5, 4.3 and 5.0 GPa. At these pressures, priderite is stable up to temperatures of 1500 °C, HAWYIM—to 1150–1300 °C and LIMA—to 1200–1350 °C (Foley et al. 1994). There is no data on the synthesis of Cr-rich priderite, which is characteristic for metasomatized peridotites. Synthetic hawthorneite and yimengite in the system TiO_2–ZrO_2–Cr_2O_3–Fe_2O_3–MgO–BaO–K_2O are stable up to 15 GPa and 1400–1500 °C, and synthetic LIMA solid solutions are stable up to 11 GPa and 1400–1600 °C (Konzett et al. 2005). The experimental data indicate a

very wide PT-range of K–Ba-titanates stability confirming the possibility of coexistence of these phases with diamond in the subcontinent upper mantle in the regions of generation of kimberlites and lamproites.

However, it is evident that not only temperature and pressure, but also specific chemical conditions are responsible for the stability of K–Ba-titanates. These minerals are formed when the ability to concentrate K and LILE in phlogopite and potassium richterite is exhausted. Formation of minerals of the HAWYIM, LIMA groups and priderite characterizes the highest degree of metasomatic changes in the conditions of high activity (concentration) of alkaline components, especially potassium in the fluids, noticeably larger than is necessary for the formation of phlogopite and potassium richterite (Safonov and Butvina 2016). The formation of these minerals is usually associated with peridotite reactions with alkali-rich fluids (melts) with low SiO_2 activity (Konzett et al. 2013; Giuliani et al 2012). The inclusions of such fluids are found in the MARID assemblages (Konzett et al. 2014), which represent the closest to those assemblages, in which K–Ba-titanates were identified. Thus, these minerals can be considered as indicators of the activity of high-alkaline aqueous-carbonic fluids or carbonate-salt melts in the upper mantle. However, there are no experimental or calculated data that would answer the question of how high the concentrations of alkali-salt components in fluids should be for the appearance of these minerals.

The paper reports results of experimental study of reactions of chromite, chromite + rutile and chromite + ilmenite forming priderite, yimengite and mathiasite with the participation of potassic aqueous-carbonic fluid at the upper-mantle P-T conditions.

9.2 Starting Materials, Experimental and Analytical Procedures

9.2.1 Starting Materials

As starting materials for experiments, mixtures (1:1 or 2:1 wt. ratios) of natural chromite with ilmenite or synthetic TiO_2 powder were used. The chromite with composition $(Mg_{0.49–0.54}Fe_{0.50–0.54}Mn_{0.01–0.02}Zn_{0.01–0.02})(Al_{0.17–0.20}Cr_{1.55–1.61}Fe_{0.10–0.22}Ti_{0.03–0.07})O_4$ (Table 1) was picked from a garnet lherzolite xenolith from the Pionerskaya kimberlite pipe, Arkhangelsk region. Ilmenite with composition $Fe_{0.98}Mg_{0.01}Mn_{0.06}Ti_{0.93}Al_{0.01}Nb_{0.01}O_3$ is a xenocrystal from the Udachnaya kimberlite pipe, Yakutia. Mixture of K_2CO_3 with oxalic acid (9:1; 7:3; 5:5; 3:7 and 1:9 ratios by weight) were used as a starting fluid component. A mixture chromite + TiO_2 was mixed with the fluid mixture as 4:1 and 9:1 by weight, whereas chromite + ilmenite as 9:1 by weight (Table 2). The starting mixtures were contained in platinum lense-like capsules with 0.2 mm wall thickness. The capsules were welded using the pulse Ar welding stage PUK-04, that allowed avoiding a loss of volatiles from the capsules.

Table 1 Chemical compositions (wt. %) of the initial minerals used in experiments on the synthesis of K-Cr titanates

Oxides	Chromite			Ilmenite	
TiO_2	1,96	1,23	2,8	46,81	45,10
Cr_2O_3	57,2	58,7	56,6	-	-
FeO*	25,7	26,4	22,9	44,25	43,39
Al_2O_3	4,10	4,24	4,80	0,78	0,25
MnO	0.75	0,18	0,58	2,99	2.65
MgO	10.10	9,49	10,50	0,58	0,49
Nb_2O_5	-	-	-	1,00	1,66
Sum	99,72	100,16	98,19	93,54	96,41
	per 4 O			**per 3 O**	
Ti	0,05	0,03	0,07	0,93	0,93
Cr	1,57	1,61	1,55	-	-
Fe^{3+}	0,15	0,15	0,10	0,09	0,07
Fe^{2+}	0,52	0,61	0,56	0,92	0,91
Al	0,18	0,17	0,20	0,03	0,05
Mn	0,02	0,01	0,02	0,06	0,06
Mg	0,53	0,49	0,54	0,03	0,02
Nb^{5+}	-	-	-	0,01	0,01

*FeO=FeO+Fe_2O_3

9.2.2 *Experimental Procedure*

The high-pressure high-temperature experiments were performed at 5 GPa and 1200 °C at the Korzhinskii Institute of Experimental Mineralogy using a toroidal anvil-with-hole apparatus of uni-axial compression by a 500-ton hydraulic press (Litvin 1991). High-pressure cells were manufactured from limestone and arranged into the space between the upper and lower anvils. Tubular heaters from graphite (length 8 mm, diameter 7.5 mm, wall thickness 0.75 mm) were disposed in the central spaces of the cells. The welded Pt capsules (diameter 4.0 mm, height 2.5 mm) with starting materials are placed at the heater centers between the electro-insulating holders being made from pressed mixtures of MgO and BN in the ratio 3:1. The temperature versus current power was calibrated using a $Pt_{70}Rh_{30}/Pt_{94}Rh_{06}$ thermocouple. The run temperatures were regulated using a MINITERM-300.31 controller with accuracy of ±0.5 °C. The quenching rate is close to 300 °C/s for the starting temperatures within 1600–1000 °C. The pressure versus press force calibration was performed against standard phase transitions in Bi (at 2.7 and 7.7 GPa) and Ba (5.5 GPa) with accuracy of 0.01–0.05 GPa (Hall 1971; Litvin et al. 1983). The accuracies of the HP-HT-experiments are estimated as ±0.1 GPa and ±20 °C, when the

P and T gradients within the cells and experimental samples are taken into account. Duration of experiments is varied (Table 2).

Oxygen fugacity was not specially controlled in the experiments being suggested that it was controlled by starting mineral phases, first of all, by chromite. The chromite composition allows estimation of $\log f_{O2}$ on the basis of the Fe^{3+}/Fe^{2+} ratio in this mineral. We used the dependence of the deviation of the oxygen fugacity of the system from the QFM buffer ($\Delta\log f_{O2}$) on the ratio Fe^{3+}/Fe^{2+} in chromite given by Nikitina et al. (2010). The Fe^{3+}/Fe^{2+} ratios in chromite were estimated from the crystal chemical formulas. The obtained values $\Delta\log f_{O2}$ (Table 3) indicate the oxygen fugacity in the experiments at 1.1–1.6 logarithmic unit below the QFM buffer.

Table 2 Run conditions and products of experiments

Run #	Starting mixture, (wt. ratio)	Fluid, (wt. ratios)	Fluid content in the system, %	Time, h.	Synthesis of priderite, yimengite, mathiasite, phlogopite
Sp1	Chromite	K_2CO_3	30	21	-,-,-, phl
Sp2	Chromite: rutile (1:1)	K_2CO_3: oxalic acid (9:1)	20	23	+,-,-, phl
A1	Chromite: rutile (1:1)	K_2CO_3: oxalic acid (9:1)	10	20	+,-,-, phl
A2	Chromite: rutile (2:1)	K_2CO_3: oxalic acid (9:1)	10	24	+,-,-, phl
B1	Chromite: ilmenite (1:1)	K_2CO_3: oxalic acid (9:1)	10	22	+,+,-, phl
B1-1	Chromite: ilmenite (1:1)	K_2CO_3: oxalic acid (7:3)	10	22	-,+,+, phl
B1-2	Chromite: ilmenite (1:1)	K_2CO_3: oxalic acid (5:5)	10	22	-,+,-, phl
B1-3	Chromite: ilmenite (1:1)	K_2CO_3: oxalic acid (3:7)	10	22	-,-,-, phl
B1-4	Chromite: ilmenite (1:1)	K_2CO_3: oxalic acid (1:9)	10	22	-,-,-, phl
B2	Chromite: ilmenite (2:1)	K_2CO_3: oxalic acid (9:1)	10	20	+,+,-, phl

Table 3 Representative analyses of chromite in the run products

№	Sp2-1	A1-1	A2-6	B1-11	B2-4
Ox/Mineral	Chr	Chr	Chr	Chr	Chr
TiO_2	2,67	3,64	3,61	4,62	4,16
Cr_2O_3	58,12	57,76	56,01	53,43	58,25
FeO	18,60	17,99	20,23	24,67	21,22
Al_2O_3	5,14	4,55	5,73	5,10	5,61
K_2O	0,24	0,20	0,10	0,38	0,20
MnO	0,60	0,29	0,81	0,39	0,61
MgO	11,51	12,42	11,92	9,61	11,48
ZnO	0,15	0,12	0,10	0,12	0,10
Sum	97,03	96,97	98,51	98,30	101,63
	Formula quantities per 3 cations				
Ti	0,07	0,09	0,09	0,12	0,10
Cr	1,57	1,56	1,49	1,45	1,51
Fe^{3+}	0,09	0,08	0,11	0,13	0,08
Fe^{2+}	0,44	0,43	0,46	0,58	0,51
Al	0,21	0,18	0,23	0,21	0,22
K	0,01	0,01	0,00	0,02	0,01
Mn	0,02	0,01	0,02	0,01	0,02
Mg	0,59	0,63	0,60	0,49	0,56
Zn	0,00	0,00	0,00	0,00	0,00
φ_{Sp}*	0,170	0,157	0,193	0,183	0,136
$\Delta \log f_{O2}$**	-1,3	-1,4	-1,1	-1,2	-1,6

*$Fe^{3+}/(Fe^{3+}+Fe^{2+})$ ratio in chromite

** $\Delta \log f_{O2} = (\log f_{O2} - \log f_{O2}^{QFM})$ (Nikitina et al., 2010)

9.3 Analytical Methods

9.3.1 Microprobe Analyses

Each run sample was embedded in epoxy and polished. After preliminary examination in reflected light, the microscopic features of run products Microprobe analyses of minerals were performed using CamScan MV2300 (VEGA TS 5130MM) electron microscope equipped with EDS INCA Energy 350 and Tescan VEGA-II XMU microscope equipped with EDS INCA Energy 450 and WDS Oxford INCA Wave 700 at the Korzhinskii Institute of Experimental Mineralogy. Analyses were performed at 20 kV accelerating voltage with a beam current up to 400 pA, spot size 115–150 nm and a zone of "excitation" of 3–4 μm diameter. Counting times was 100 s for all elements. The ZAF matrix correction was applied.

9.3.2 Raman Spectroscopy

The Raman spectra were obtained using the Renishaw RM1000 microscope/spectrometer equipped with the diode-pumped modular laser 532 nm. The typical parameters of measurements are following: laser output power 22 mW, slit 50 mm, collection time 100 s. The alignment of the spectrometer was checked before run by taking spectra of high-purity monocrystalline Si.

9.4 Experimental Results

9.4.1 Phase Relations

Natural Cr-rich K–Ba-titanates are closely related to chromite. Therefore, in order to find out a possibility for formation of any of these phases in direct interaction of chromite with the potassic fluid, an experiment with a mixture of chromite with K_2CO_3 (run Sp1; Table 2) has been performed. However, no any potassium-bearing phases were identified in the products of this experiment. The principal conclusion from this experiment is necessity of additional Ti-bearing phases which associated with chromite for the formation of titanates.

In fact, interaction of chromite with the K_2CO_3–H_2O–CO_2 fluid in presence of rutile (runs Sp2, A1, A2; Table 2) resulted in formation of priderite. It forms individual anhedral and subhedral grains, as well as tetragonal prisms and di-tetragonal dipyramids up to 40 μm in size (Figs. 1 and 2a). Priderite also forms inclusions in rutile (Fig. 2b). Formation of priderite results in changes in the chromite composition, which becomes poorer in FeO + Fe_2O_3 and Cr_2O_3, but richer in TiO_2 compared to the starting chromite (Table 1). Using composition of phases in the run Sp2 products

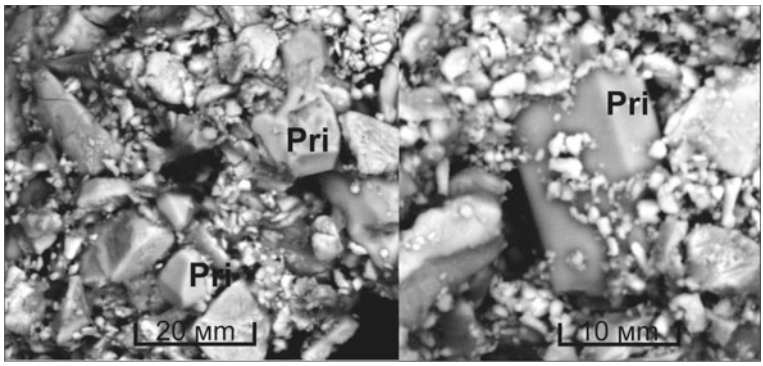

Fig. 1 Tetragonal crystals of priderite (run A, Table 2) in the system chromite-rutile-K_2CO_3–H_2O–CO_2 at 5 GPa and 1200 °C

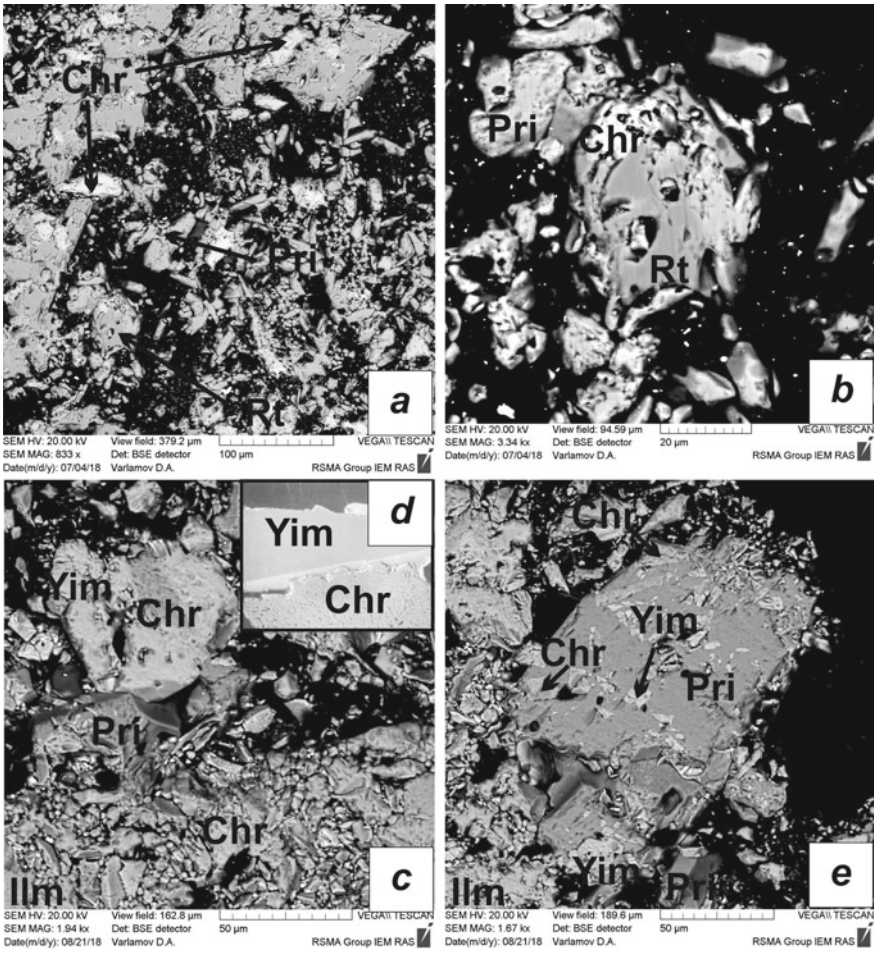

Fig. 2 Run products of the experiment B1 (Table 2) in the system chromite-rutile/ilmenite-K_2CO_3–H_2O–CO_2 at 5 GPa and 1200 °C. **a**, **b** Experiments A1 and A2 (Table 2): priderite, chromite, rutile; **c**, **e** experiment B1 (Tables 2 and 5): chromite, ilmenite, priderite, yimengite; **d** intergrowth of yimengite and chromite from the kimberlite sill Prospect 039, Guaniamo province, Venezuela (Nixon, Condliffe, 1989)

(Table 5), the following equilibrium represents the formation of priderite:

$$24.50\mathrm{Chr}_2 + 5.79\mathrm{TiO}_2 + \mathrm{K}_2\mathrm{CO}_3 + 0.46\mathrm{O}_2 + 1.10\mathrm{Cr}_2\mathrm{O}_3 = 1.17\mathrm{Pri} + 9.45\mathrm{Chr} + 14.57\mathrm{Chr}_1 + \mathrm{CO}_2 \quad (1)$$

The equilibrium demonstrates formation of priderite with variations of the chromite composition. Slight oxidation is needed to accommodate Fe^{3+} in the forming priderite. Some excess of Cr_2O_3 demonstrates either non-stoicheometry of priderite or formation of additional oxides in the run products. In fact, some grains of unidentified Cr and Ti-bearing oxides were detected in the run products.

Other titanates are absent in the runs with rutile at any chromite/rutile ratios. The possible reason is an insufficient amount of Fe, first of all, Fe^{3+}. This suggestion is supported by the experiments in the chromite-ilmenite-K_2CO_3–H_2O–CO_2 system (runs B1, B1-1, B1-2, B1-3, B1-4, B2; Table 2). Products of these experiments contain yimengite along with priderite. The titanates are associated with chromite, ilmenite, as well as with newly formed rutile (compositions see in Table 4). Anhedral or subhedral grains of priderite of 10–100 μm in size locally contain inclusions of chromite and ilmenite. Yimengite is also found as inclusions in priderite (Fig. 2e). This phase forms intergrowths with chromite, which closely resemble natural examples (Nixon and Condliffe 1989) (Fig. 2c, d). The chromite/ilmenite ratio does not influence on the titanate crystallization.

However, their formation is affected by the $K_2CO_3/(H_2O + CO_2)$ ratio in the starting fluid mixture at the constant fluid content in the system. Experiments of the series B1, B1-1, B1-2, B1-3, B1-4 and B2 (Table 2) were performed using starting mixtures with variable wt. $K_2CO_3/(H_2O + CO_2)$ ratios and allowed evaluation of a sequence of the formation of various K–Cr-titanates and their assemblages on the fluid composition (Table 2). The assemblage priderite + yimengite form at the ratio $K_2CO_3/(H_2O + CO_2) = 9/1$ (Table 2). Using composition of phases in the run B1 products (Table 2), a number of equilibria could be written to illustrate the formation of this titanate assemblage, for example:

$$\begin{aligned} \mathrm{Rt} + 0.11\mathrm{Chr} + 0.12\mathrm{K_2CO_3} + 0.21\mathrm{Ilm_1} &= 0.11\mathrm{Pri} + 0.05\mathrm{Yim} \\ &+ 0.03\mathrm{Cr_2O_3} + 0.13\mathrm{Ilm_2} + \mathrm{CO_2} \end{aligned} \quad (2)$$

The equilibrium demonstrates formation of priderite and yimengite with variations of the ilmenite composition. Again, slight excess of Cr_2O_3 demonstrates either non-stoicheometry of titanates or formation of additional oxides in the run products. In fact, some grains of Cr-bearing (0.2 a.p.f.u.) rutile were detected in the run products.

Decrease of the ratio $K_2CO_3/(H_2O + CO_2)$ to 7/3 leads to disappearance of priderite, but yimengite actively forms as subhedral hexagonal crystals of 10–100 μm in size (Fig. 3). K-poor titanate, mathiasite, appears along with yimengite. Yimengite only forms at $K_2CO_3/(H_2O + CO_2) = 5/5$. Using representative composition of phases in the run B1-1 products (Table 2), a number of equilibria could be written to illustrate the formation of this titanate assemblage, for example:

$$\begin{aligned} 5.29\mathrm{Chr} + 9.87\mathrm{Ilm} + 1.08\mathrm{K_2CO_3} + 7.61\mathrm{TiO_2} \\ = \mathrm{Yim_1} + 1.14\mathrm{Yim_2} + 0.68\mathrm{Cr_2O_3} + 8.09\mathrm{Ilm_3} \end{aligned} \quad (3)$$

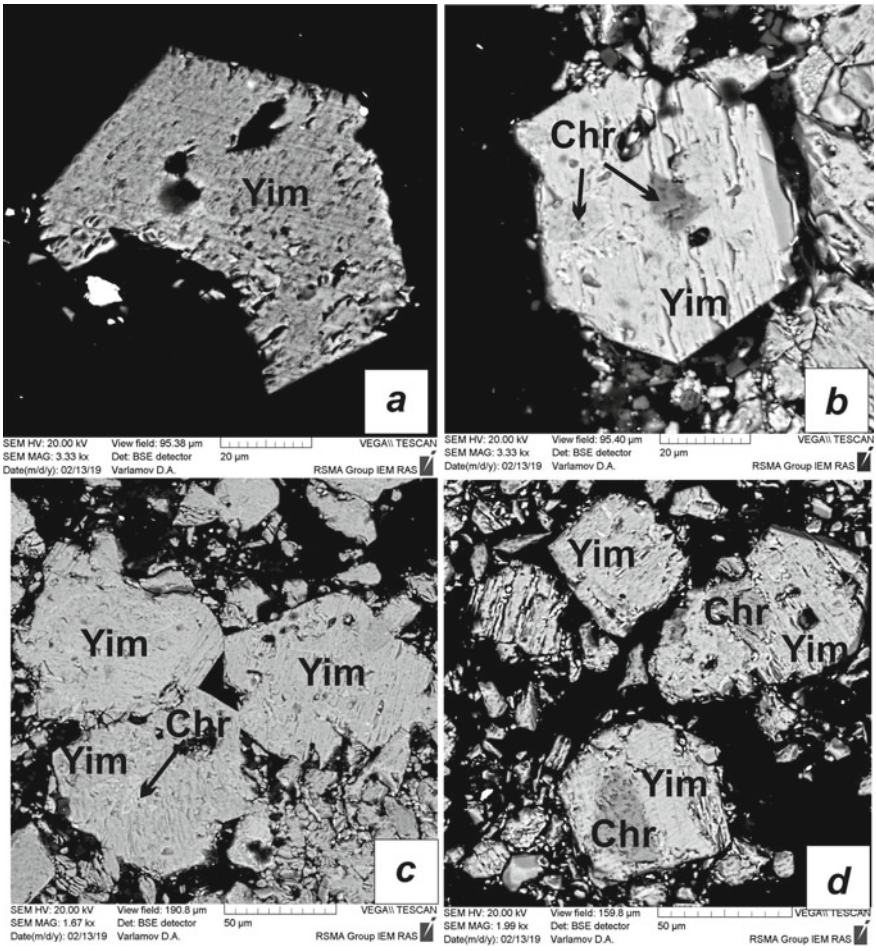

Fig. 3 Products of the experiment B1-1 and B1-2 (Table 2) in the system chromite-ilmenite-K_2CO_3–H_2O–CO_2 at 5 GPa and 1200 °C: hexagonal crystals of yimengite

The equilibrium demonstrates formation of yimengite with variations of the ilmenite composition (it becomes more magnesian). The excess of Cr_2O_3 and TiO_2 demonstrates possible non-stoicheometry of titanates or formation of additional non-detectible oxides in the run products.

No titanates are observed at lower $K_2CO_3/(H_2O + CO_2)$ ratios (Table 2).

The products of all experiments contain some phlogopite, which was formed, probably, due to a presence of various silicate phases – inclusions or intergrowths in the starting ilmenite and chromite. Usually, it forms aggregates between grains of starting and newly formed phases being closely associated with K-bearing titanates (Fig. 4). However, phlogopite is present even in run products, which do not contain titanates (experiments Sp1, B1-3 and B1-4; Table 2).

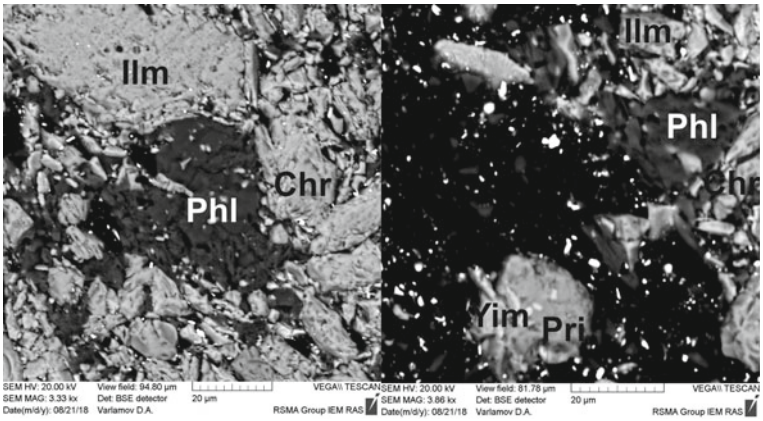

Fig. 4 Products of experiment B2 (Table 2) in the system chromite-ilmenite-K_2CO_3–H_2O–CO_2 at 5 GPa and 1200 °C containing phlogopite

9.4.2 Phase Compositions

Representative microprobe analyses of synthesized titanates are given in Tables 4 and 5. The ratios of Fe ($Fe^{2+} + Fe^{3+}$), Ti and Cr in formulas of priderite synthesized in systems both with rutile and ilmenite differ insignificantly (Fig. 5). Compositions of yimengite produced in the reactions of chromite and ilmenite with the fluid form the trend, which reflect the isomorphism ($Fe^{2+} + Fe^{3+}$) + Ti ↔ Cr at the nearly constant ($Fe^{2+} + Fe^{3+}$)/Ti ratio (Fig. 5). Yimengite is characterized by a relatively low content of Al_2O_3 and MgO. It contains up to 3.5 wt% Nb_2O_5, despite the fact that coexisting priderite does not contain this component (Tables 4 and 5).

Phlogopite in the run products contains 0.6–1.9 wt% TiO_2 and 1.8–2.7 wt% Cr_2O_3 reflecting its formation in the reactions involving both chromite and ilmenite or rutile. In the series of experiments with variable $K_2CO_3/(H_2O + CO_2)$ ratio (series B in Table 2), the highest concentrations of these components are detected in phlogopites forming in the reactions with fluids with high $K_2CO_3/(H_2O + CO_2)$ ratio (9:1 and 7:3) suggesting more active involvement of chromite and ilmenite in the phlogopite-forming reactions.

9.4.3 Raman Spectra of Titanates

The presence of priderite, yimengite and mathiasite was confirmed using Raman spectroscopy. Raman spectra of Cr-bearing priderite within the range of 150–1200 cm^{-1} (Fig. 6) are characterized by three intense bands at 159, 359 and 692 cm^{-1} (Fig. 6 **I**), close to those for the spectra of natural K–Cr-priderite (Konzett et al. 2013; Naemura et al. 2015). However, in contrast to the spectra of natural K–Cr-priderite,

Table 4 Representative analyses of priderite, yimengite and mathiasite

№№	Sp-4	Sp-5	A1-5	A2-7	B1-12	B1-3	B1-1-2	B1-1-12
Минерал	Pri	Pri	Pri	Pri	Yim	Yim	Yim	Ma
TiO_2	69,45	69,03	69,83	69,21	34,29	38,34	36,11	51,16
Cr_2O_3	15,62	16,45	19,00	17,03	25,31	21,9	23,14	2,29
FeO*	0,83	0,5	0,52	0,42	23,09	26,3	24,4	32,42
Al_2O_3	0,91	0,89	0,79	0,70	1,97	1,68	1,56	0,39
K_2O	11,26	11,39	10,95	11,26	4,78	4,88	5,15	1,89
MnO	0,37	0,03	0,15	0,06	1,79	1,80	1,68	2,82
MgO	0,68	0,51	0,30	0,40	2,20	1,82	2,27	5,36
Nb_2O_5	0,00	0,00	0,00	0,12	2,94	3,44	2,35	2,00
Сумма	99,12	98,80	101,54	99,20	96,37	100,16	96,66	98,33
	Per 16 O				**Per 19 O**			**Per 38 O**
Ti	6,23	6,22	6,13	6,22	4,04	4,34	4,23	12,05
Cr	1,47	1,56	1,75	1,61	3,14	2,60	2,85	0,57
Fe^{3+}	0,07	0,05	0,05	0,04	2,24	2,41	2,47	8,48
Fe^{2+}	-	-	-	-	0,48	0,57	0,39	-
Al	0,13	0,13	0,11	0,10	0,36	0,30	0,29	0,14
K	1,71	1,74	1,63	1,72	0,96	0,94	1,02	0,75
Mn	0,04	0,00	0,01	0,01	0,24	0,23	0,22	0,75
Mg	0,12	0,09	0,05	0,07	0,51	0,41	0,53	2,50
Nb^{5+}	0,00	0,00	0,00	0,01	0,24	0,27	0,19	0,28

*$FeO=FeO+Fe_2O_3$

the main bands in the spectra of the synthetic priderite are noticeably shifted to higher wave numbers. This is probably due to the lack of Ba in the synthetic priderite.

Raman spectra of yimengite (Fig. 6 **II**) show intense bands at 378, 508, 682 and 757 cm^{-1}, consistent with the spectra of the synthetic HAWYIM solid solution (Konzett et al. 2005). In comparison to the HAWYIM solid solution (Konzett et al. 2005), the bands in the spectra of the synthesized yimengite are shifted to higher wave numbers. As in the case of priderite, the shift of the bands, apparently, is associated with the absence of Ba in the composition of yimengite.

Raman spectra of mathiasite (Fig. 6 **III**) are characterized by intense peaks at 258, 332, 456, 587, 682 cm^{-1}, consistent with the spectra of the synthetic LIMA solid solution (bands at 243, 327, 433, 560 and 661–702 cm^{-1}) (Konzett et al. 2005). The shift by 5–20 cm^{-1} of all bands can be explained by different contents of the end-members of lindsleyite, loveringite (Ca-containing end-member) and mathiasite in the crichtonite phase.

Table 5 Representative compositions (a.p.f.u.) of coexisting phases in some run products

Run #	B1				
a.p.f.u./mineral	Yim	Pri	Ilm_1	Ilm_2	Rt
Ti	4,76	6,15	0,93	0,98	0,85
Cr	2,87	1,56	-	0,01	0,20
Fe^{3+}	0,25	0,15	0,08	0,03	-
Fe^{2+}	3,30	0,10	0,95	0,70	-
Al	0,35	0,06	0,02	-	-
K	1,01	1,77	-	-	-
Mg	0,47	0,06	0,04	0,28	-

Run #	Sp2			B1-1		
a.p.f.u./mineral	Chr_1	Chr_2	Pri	Yim_1	Yim_2	Ilm_3
Ti	0,10	0,14	6,23	4,34	4,25	0,97
Cr	1,47	1,46	1,47	2,99	3,31	0,02
Fe^{3+}	0,02	-	0,11	0,68	0,42	0,04
Fe^{2+}	0,31	0,46	-	2,61	2,74	0,74
Al	0,31	0,26	0,13	0,69	0,66	-
K	-	-	1,71	1,00	1,01	-
Mg	0,79	0,68	0,12	0,67	0,67	0,23

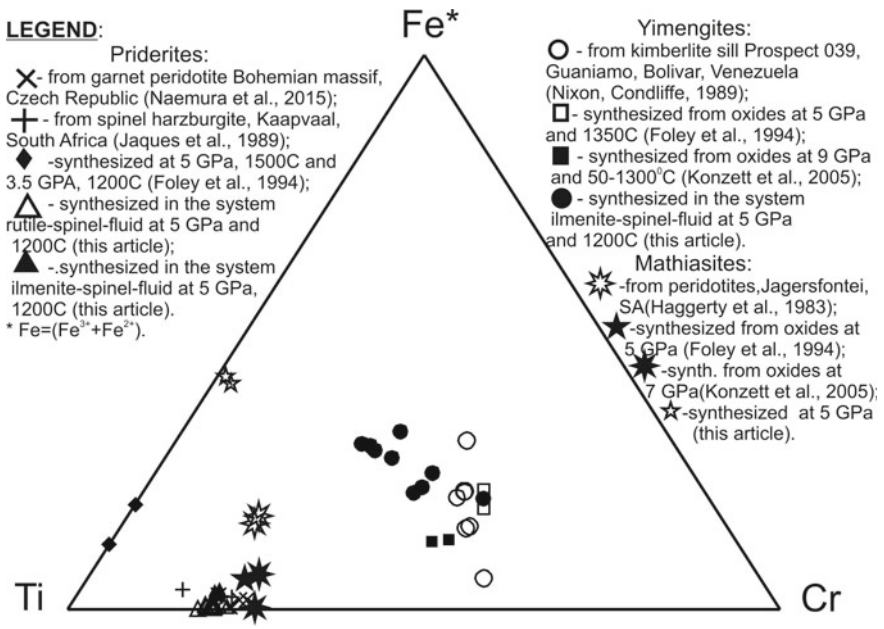

Fig. 5 Diagram of Ti – Fe – Cr illustrating the variation of the composition of synthesized yimengite, mathiasite and priderite in comparison with the compositions of natural minerals

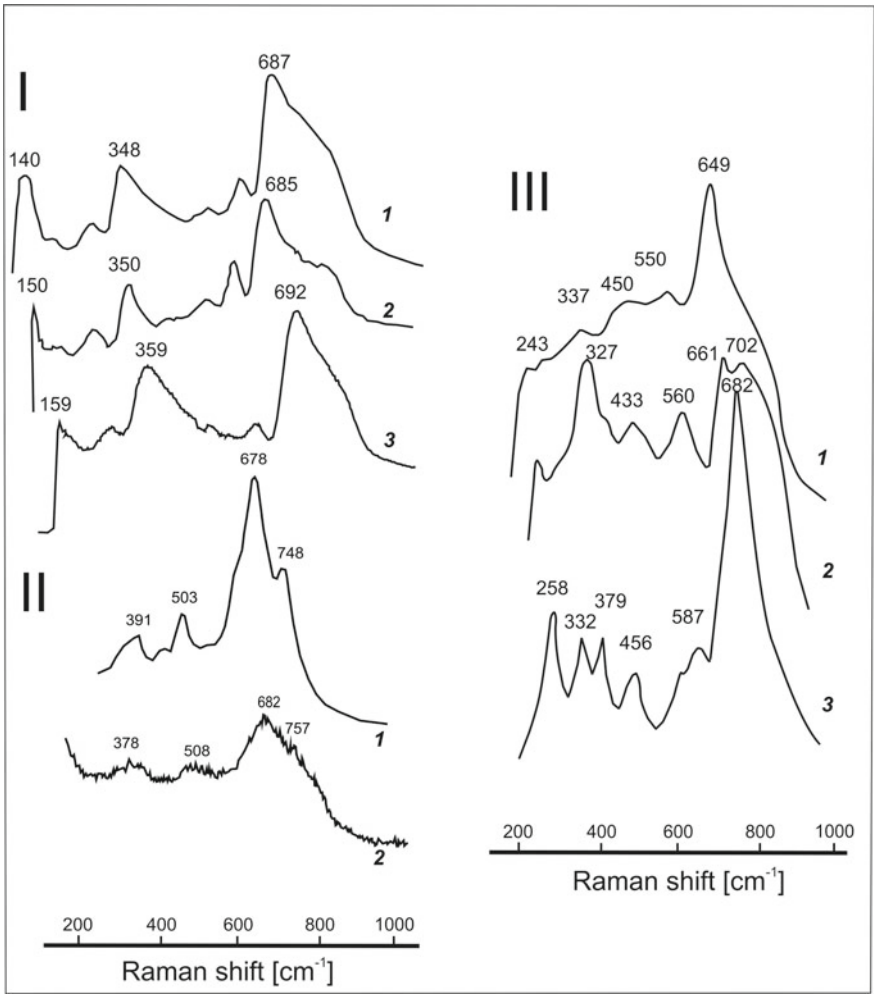

Fig. 6 Raman spectra of the synthesized phases: (I-1) K-Cr priderite from metasomatized peridotites from kimberlites of South Africa (Konzett et al. 2013); (I-2) K-Ba-Cr priderite from inclusions in chromites of Bohemian Massif garnet peridotites (Naemura et al. 2015); (I-3) synthesized K-Cr priderite (analysis Sp-4, Table 4); (II-1) solid solution yimengite-hawthorneite synthesized from the oxides at 12 GPa and 1400 °C (ex. JKW88, see Konzett et al. 2005); (II-2) the synthesized yimengite (analysis B1-12, Table 4); (III-1) mathiasite synthesized from the oxides at 7 GPa and 1300 °C (ex. JKW43, see Konzett et al. 2005); (III-2) lindsleyite synthesized from the oxides at 7 GPa and 1300 °C (ex. JKW43, see Konzett et al. 2005); (III-3) synthesized mathiasite (analysis B1-1-12, Table 4)

9.5 Discussion

Experimental data on synthesis of K–Ba-titanates demonstrate that there are virtually no restrictions on their stability at the upper-mantle and, possibly, transition zone PT-conditions (Podpora and Lindsley 1984; Foley et al. 1994; Konzett et al. 2005). The main restriction is imposed by the compositional characteristics of the mantle protolith and fluids, whose reactions produce these minerals.

Petrological and mineralogical studies of mantle xenoliths show that the predominant type of mantle protolith for the formation of Cr-bearing K–Ba-titanates are peridotites enriched in Cr_2O_3, but rather poor in Al_2O_3. These are subcratonic depleted harzburgites. However, K–Ba-titanates are known in lherzolite assemblages, as well (e.g. Rezvukhin et al. 2018). The formation of Cr-rich K–Ba-titanates is usually associated with reactions of chromite in peridotites with fluids or melts enriched in potassium and incompatible elements (e.g. Haggerty et al. 1983; Haggerty 1983; Nixon and Condliffe 1989; Sobolev et al. 1998; Bulanova et al. 2004; Rezvukhin et al. 2018). The phase relations in the run products clearly showed this process (Figs. 2a–e and 3b, d). However, experiments also showed that these phases did not form after chromite directly, but demanded an additional source of titanium. This source cannot be depleted peridotites usually containing less than 0.1 wt% TiO_2 (e.g. Rudnick et al. 1998). Many authors pay attention to elevated TiO_2 content (up to 7 wt%) of chromite associated with K–Ba titanates (Zhou 1986; Nixon and Condliffe 1989; Bulanova et al. 2004), which is atypical for chromite in the subcratonic peridotites. Of course, this compositional feature is related to the preliminary interaction of chromite with metasomatizing fluids/melts, which introduce Ti and incompatible elements. Such interaction results in not only the enrichment of chromite in titanium, but also in the formation of ilmenite and rutile, which subsequently serve as reagents for the formation of titanates (Konzett et al. 2000; Almeida et al. 2014). For example, lindsleyite-mathiasite reaction on Cr-bearing ilmenite, which is itself a product of the metasomatism, has been described in xenoliths from South African kimberlites (Konzett et al. 2000). It cannot be excluded that the suppliers of titanium for the K–Ba-titanate-forming reactions may be garnet and clinopyroxene, which are capable to contain high concentrations of both titanium and chromium, especially at high pressures (e.g. Zhang et al. 2003). However, this conclusion requires experimental confirmation, since there are no experiments on crystallization of K–Ba-titanates in the presence of chromium and titanium-bearing silicates. Natural assemblages also do not provide evidence for the formation of these phases after garnet and pyroxenes, although the inclusions of the crichtonite group minerals in chromium pyropes are known (Wang et al. 1999; Rezvukhin et al. 2018). It is possible that the absence of such evidence is explicable by the specificity of mantle metasomatism. During the processes of modal mantle metasomatism of peridotites with the participation of alkaline fluids, garnet, as a rule, disappears quickly during the phlogopite and/or potassium richterite-forming reactions (Safonov and Butvina 2016). In addition to limited substitution into hydrous aluminosilicates (phlogopite and amphibole), Cr from garnet forms a new chromium-bearing spinel. This spinel can also serve a

reagent for the formation of Cr-bearing K–Ba-titanates in the subsequent stages of metasomatic transformations.

Phlogopite and potassium richterite are typical products of modal mantle metasomatism, during which K–Ba-titanates form. Their formation is determined not only by the potassium content in the system, but also by the ratio of its content to the activity of water in fluids. Hydrous aluminosilicates are not only active containers of potassium and other LILE, but also able to accommodate Cr and Ti. Thus, phlogopite and potassium richterite can act as contenders for K–Ba-titanates. Cr and Ti-rich phlogopite was identified in the products of all experiments (Table 2 and Fig. 4). It appears even in experiments where K-titanates are not detected (experiments B1-3 and B1-4). These experiments are characterized by the lowest $K_2CO_3/(H_2O + CO_2)$ ratios in the starting fluid mixture (3:7 and 1:9, respectively). This result is consistent with experimental data on the interaction of peridotites with K_2CO_3 and KCl-bearing fluids (Edgar and Arima 1984; Thibault and Edgar 1990; Safonov and Butvina 2013; Sokol et al. 2015), which demonstrate that phlogopite is formed in a wide range of H_2O/salt ratios, from undersaturated water-salt fluids to hydrous salt melts. Thermodynamic calculations show that phlogopite in peridotite assemblages is formed at water activities down to values of 0.1, and potassium activity is the leading factor determining the formation of this mineral (Safonov and Butvina 2016). In experiments with higher $K_2CO_3/(H_2O + CO_2)$ ratios in starting fluids, phlogopite coexists with Cr-bearing K-titanates. This means that the crystallization of titanates together with phlogopite is determined not so much by the activity of water as by the activity of the potassium component of the fluid. The close natural association of titanates with phlogopite and/or K-amphibole indicates that the formation of HAWYIM and LIMA minerals and priderite is possible at excess of potassium and other LILE, when the mineral capacity of the system relative to these components exceeds the possibility for mica and amphibole formation (Konzett et al. 2005; Safonov and Butvina 2016). Reactions of phlogopite with relic Cr-rich spinel can form K-bearing titanates at the advanced stage of metasomatic processes (e.g. Almeida et al. 2014).

High potassium activity in the mineral-forming medium, necessary for the formation of Cr-bearing K–Ba-titanates, corresponds to the highest degrees of metasomatism. Such conditions can be created either with a continuous and intensive interaction of ultrapotassic fluids/melts with rocks, or during a multi-stage process with an increasing effect. For example, two-stage metasomatic process is described by Konzett et al. (2013) in the spinel harzburgites from kimberlites of South Africa. The first stage of metasomatic transformation results in the formation of phlogopite, K-amphibole, titaniferous phase (rutile and srilankite) and crichtonite phase (mathiasite). The subsequent stage of metasomatism is manifested by the decomposition of these minerals to form new generations of amphibole, phlogopite, clinopyroxene, olivine, various rare Ti and Zr-bearing minerals. In this association, Cr-rich priderite replaces mathiasite. The authors believe that the second stage of metasomatism was due to the interaction of rocks with ultra-alkaline fluids/melts with low silica activity (Konzett et al. 2013), which is typical for alkaline carbonatite melts. The relics of such melts have been repeatedly described as polymineral inclusions in kimberlite minerals, including diamonds, minerals of peridotite xenoliths in kimberlites, as well as in

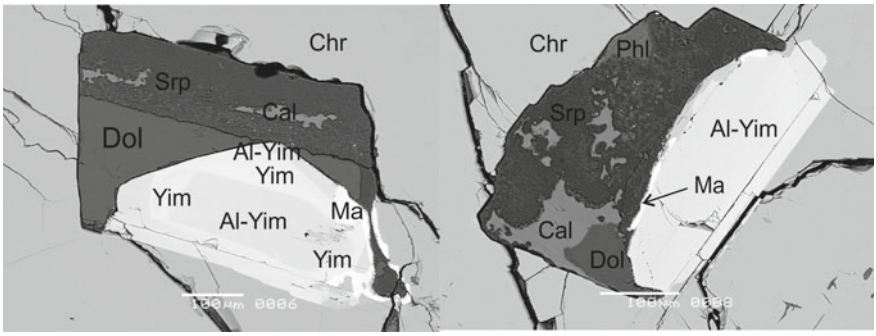

Fig. 7 Polyphase inclusions in chromite: yimengite, Al-rich yimengite, mathiasite, dolomite, calcite, serpentine and phlogopite. BSE image

minerals of alpine-type orogenic peridotites. Associations of these inclusions consist of mixtures of carbonate and silicate minerals with phosphate, sulfide, chloride, sulfate and other phases reflecting the complex composition of the trapped carbonatite melts. Among phases composing the polymineral inclusions, K–Ba titanates were described. Priderite has been discovered in carbonate-silicate inclusions in chromite of garnet peridotite in the Bohemian massif (Naemura et al. 2015) and in ilmenites of the Bultfontein kimberlite pipe, South Africa (Giuliani et al. 2012). The crichtonite group minerals were found in carbonate-bearing polyphase inclusions in chromium pyropes from the International kimberlite pipe, Yakutia (Rezvukhin et al. 2018). Figure 7 shows large polyphase inclusions in chromite from garnet lherzolite xenolith from the Obnazhennaya kimberlite pipe, Yakutia. They contain yimengite. Subhedral outlines of the yimengite crystals manifest a free growth of mineral within the inclusions. Zoning in these crystals (Fig. 7) is resulted from the alternation of zones with different Al/Cr ratios. Yimengite is associated with dolomite, phlogopite, serpentine and calcite (probably, products of a later reaction inside the inclusions on cooling $6Dol + 4H_2O + 4SiO_2 = 2Srp + 6Cal + 6CO_2$). The presence of phlogopite and yimengite indicates a high primary content of potassium in the inclusions. It is evident that the inclusions are relics of solidified alkaline hydrous carbonate-silicate melts, the interaction of which with the host chromite led to the formation of titanates.

The experiments confirmed the possibility of joint formation of different titanates as a result of the interaction of chromite and ilmenite with potassic aqueous carbonate fluid/melt with different $K_2CO_3/(H_2O + CO_2)$ ratios. Associations containing two different titanates are known in metasomatized xenoliths. In these cases, reaction relationships between titanates are usually observed. Replacement of yimengite by priderite were described in xenoliths from Chinese kimberlites (Zhou 1986). In the above-mentioned xenoliths of spinel harzburgites from South African kimberlites (Konzett et al. 2013), priderite was produced during the repeated stage of metasomatism and replaced the LIMA phases. The authors conclude that the second stage of metasomatism was due to the interaction of rocks with fluids characterized by higher potassium activity (Konzett et al. 2013). Almeida et al. (2014) concluded that

priderite-bearing xenoliths record an action of more potassic metasomatizing melts than mathiasite-bearing xenoliths. These observations and conclusions are in good agreement with the observed sequence of appearance of various titanates depending on the $K_2CO_3/(H_2O + CO_2)$ ratio. Priderite appears at a higher ratio, which corresponds to higher potassium activity. In the above-mentioned polyphase inclusions in chromite from garnet lherzolite xenolith, crystals of yimengite are replaced by thin bay-shaped edges of mathiasite (Fig. 7). Following to the experiments, the association yimengite + mathiasite appears during the reaction of chromite and ilmenite with the fluid with higher $K_2CO_3/(H_2O + CO_2)$ ratio than yimengite alone. With application to the polyphase inclusions, the replacement of yimengite by mathiasite can be interpreted as the result of an accumulation of potassium component of the fluid/melt by crystallization within the inclusion and interaction with the chromite host.

9.6 Conclusions

Experiments on the interaction of chromite + rutile and chromite + ilmenite associations in the presence of a small amount of silicate material with H_2O–CO_2–K_2CO_3 fluids at 5 GPa revealed the following features of crystallization of titanate minerals and allowed interpretation of their associations in metasomatized mantle peridotites.

(1) The principal possibility of the formation of minerals of crichtonite and magnetoplumbite groups and priderite in the reactions of chromite with alkaline aqueous-carbonic fluids and melts is confirmed. Such substances are considered as main agents of potassium metasomatism, leading to the formation of titanates in the upper mantle (Konzett et al. 2013; Rezvukhin et al. 2018).

(2) The formation of these phases does not proceed directly on chromite (e.g. Haggerty et al. 1983; Haggerty 1983; Nixon and Condliffe 1989), and requires additional titanium source. They are rutile and ilmenite, which are themselves usually are products of modal metasomatism of peridotites. This experimental fact demonstrates that the formation of titanates marks probably the most advanced or repeated stages of metasomatism in mantle peridotites.

(3) This is also proved by the relationships of titanates with phlogopite. Association of titanates with phlogopite is characterized by a higher activity of the potassium component in the fluid/melt than the formation of phlogopite alone. Such conditions can again be created at the most advanced or repeated stages of mantle metasomatism.

(4) The relationship between titanates is also a function of the activity of the potassium component in the fluid/melt. Priderite is an indicator of the highest potassium activity in the mineral-forming medium. The above examples from natural associations (Zhou 1986; Konzett et al. 2013; Almeida et al. 2014) well illustrate this conclusion.

Acknowledgements The work was financially supported by the governmental projects AAAAA18-118020590148-3 and AAAA-A18-118020590140-7 of the Korzhinskii Institute of Experimental Mineralogy.

References

Almeida V, Janasi V, Svisero D, Nannini F (2014) Mathiasite-loveringite and priderite in mantle xenoliths from the Alto Paranaíba Igneous Province, Brazil: genesis and constraints on mantle metasomatism. Open Geosci 6(4):614–632

Bailey DK (1982) Mantle metasomatism—Continued chemical change within the Earth. Nature 296:525–580

Bailey DK (1987) Mantle metasomatism–perspective and prospect. In: Fitton JG, Upton BGJ (eds) Alkaline igneous rocks, vol 30. Geological Society Special Publication, pp 1–13

Bulanova GP, Muchemwa E, Pearson DG, Griffin BJ, Kelley SP, Klemme S, Smith CB (2004) Syngenetic inclusions of yimengite in diamond from Sese kimberlite (Zimbabwe)—evidence for metasomatic conditions of growth. Lithos 77(1–4):181–192

Dong Z, Zhou J, Lu Q, Peng Z (1983) Yimengite, $K(Cr, Ti, Fe, Mg)_{12}O_{19}$, a new mineral from China. Kexue Tongbao Bull Sci 15:932–936 (in Chinese)

Edgar AD, Arima M (1984) Experimental studies on K-metasomatism of a model pyrolite mantle and their bearing on the genesis of uitrapotassic magmas. In: Proceedings of 27th International Geological Congress Petroleum (Igneous and metamorphic rocks), vol 9, pp 509–541

Erlank AJ, Rickard RS (1977) Potassic richterite bearing peridotites from kimberlite and the evidence they provide for upper mantle metasomatism. (Abstract) Second International Kimberlite Conference, Santa Fe, New Mexico

Foley S, Hofer H, Brey G (1994) High-pressure synthesis of priderite and members of lindsleyite-mathiasite and hawthorneite-yimengite series. Contrib Mineral Petrol 117:164–174

Giuliani A, Kamenetsky VS, Phillips D, Kendrick MA, Wyatt BA, Goemann K (2012) Nature of alkali-carbonate fluids in the sub-continental lithospheric mantle. Geology 40(11):967–970

Grey IE, Madsen IC, Haggerty SE (1987) Structure of a new upper-mantle magnetoplumbite-type phase, $Ba(Ti_3Cr_4Fe_4Mg)O_{19}$. Am Mineral 72:633–636

Haggerty SE (1975) The chemistry and genesis of opaque minerals in kimberlites. Phys Chem Earth 9:295–307

Haggerty SE (1983) The mineral chemistry of new titanates from the Jagersfontein kimberlite, South Africa: implications for metasomatism in the upper mantle. Geochim Cosmochim Acta 47(11):1833–1854

Haggerty SE (1987) Metasomatic mineral titanates in upper mantle xenoliths. In: Nixon PH (ed) mantle xenoliths. Wiley, Chichester, pp 90–671

Haggerty SE (1991) Oxide mineralogy of the upper mantle. In: Lindsley DH (eds) Oxide minerals: Petrologic and magnetic significance. Rev Mineral 25: 355–416

Haggerty SE, Smyth JR, Erlank AJ, Rickard RS, Danchin RV (1983) Lindsleyite (Ba) and mathiasite (K): two new chromium-titanates in the crichtonite series from the upper mantle. Am Mineral 68:494–505

Haggerty SE, Erlank AJ, Grey IE (1986) Metasomatic mineral titanate complexing in the upper mantle. Nature 319(6056):761–763

Haggerty SE, Grey IE, Madsen IC, Criddle AJ, Stanley CJ, Erlank AJ (1989) Hawthorneite, $Ba[Ti_3Cr_4Fe_4Mg]O_{19}$: a new metasomatic magnetoblumbite-type mineral from the upper mantle. Am Mineral 74:668–675

Hall HT (1971) Fixed points near room temperature: accurate characterization of the high pressure environment. National Bureau of Standards. US. Spec. Publ. №. 326, Washington, DC, p 313

Harte B (1983) Mantle peridotites and processes—The kimberlite sample. In: Hawkesworth CJ, Norry MJ (eds) Continental basalts and mantle xenoliths. Shiva, Cheshire, pp 46–91

Harte B, Gurney JJ (1975) Ore mineral and phlogopite mineralization within ultramafic nodules from the Matsoku kimberlite pipe, Lesotho, vol 74. Carnegie Inst Yearbook, Washington, pp 528–536

Jaques AL, Hall AE, Sheraton JW, Smith CB, Sun SS, Drew RM, Foudoulis C, Ellingsen K (1989) Composition of crystalline inclusions and C-isotopic composition of Argyle and Ellendale diamonds. In: Jaques AL, F'erguson J, Green DH (eds) Kimberlites and related rocks 2: their crust/mantle setting, diamonds, and diamond exploration. Blackwells, Melbourne, pp 966–989

Jones AP, Smith JV, Dawson JB (1982) Mantle metasomatism in 14 veined peridotites from Bultfontein Mine, South Africa. J Geol 435–453

Kiviets GB, Phillips D, Shee SR, Vercoe SC, Barton ES, Smith CB, Fourie LF (1998) 40Ar/39Ar dating of yimengite from Turkey Well kimberlite, Australia: the oldest and the rarest. In: 7th International Kimberlite Conference, pp 432–434

Konzett J, Armstrong RA, Günther D (2000) Modal metasomatism in the Kaapvaal craton lithosphere: Constraints on timing and genesis from U-Pb zircon dating of metasomatized peridotites and MARID-type xenoliths. Contrib Mineral Petrol 139(6):704–719

Konzett J, Yang H, Frost DJ (2005) Phase relations and stability of magnetoplumbite- and crichtoniteseries phases under upper-mantle P-T conditions: an experimental study to 15 GPa with implications for LILE metasomatism in the lithospheric mantle. J Petrol 46(4):749–781

Konzett J, Wirth R, Hauzenberger C, Whitehouse M (2013) Two episodes of fluid migration in the Kaapvaal Craton lithospheric mantle associated with Cretaceous kimberlite activity: evidence from a harzburgite containing a unique assemblage of metasomatic zirconium-phases. Lithos 182:165–184

Konzett J, Krenn K, Rubatto D, Hauzenberger C, Stalder R (2014) The formation of saline mantle fluids by open-system crystallization of hydrous silicate–rich vein assemblages—evidence from fluid inclusions and their host phases in MARID xenoliths from the central Kaapvaal Craton, South Africa. Geochim Cosmochim Acta 147:1–25

Litvin YA (1991) Physico-chemical studies of the melting of the earth's deep matter. Science, Moscow, 312 p (in Russian)

Litvin YA, Livshits LD, Karasev VV, Chudinovskikh LT (1983) On reliability of experiments and P-T measurements at studies of physico-chemical equilibria in the solid-phase apparatuses. Phys Techn High Press 14:50–56

Lloyd FE, Bailey DK (1975) Light element metasomatism of the continental mantle: the evidence and the consequences. Phys Chem Earth 9:389–416

Menzies MA, Hawkesworth CJ (1987) Mantle metasomatism. Academic Press, London

Naemura K, Shimizu I, Svojtka M, Hirajima T (2015) Accessory priderite and burbanrite in multiphase solid inclusions in the orogenic garnet peridotite from the Bohemian Massif, Czech Republic. Mineral Petrol 110:20–28

Nikitina LP, Goncharov AG, Saltykova AK, Babushkina MS (2010) The redox state of the continental lithospheric mantle of the Baikal-Mongolia region. Geochem Int 48(1):15–40

Nixon PH, Condliffe E (1989) Yimengite of K-Ti metasomatic origin in kimberlitic rocks from Venezuela. Min Mag 53:305–309

Norrish K (1951) Priderite, a new mineral from the leucite lamproites of the West Kimberley area, Western Australia. Min Mag 73:1007–1024

Peng Z, Lu Q (1985) The crystal structure of yimengite. Sci Sinica (Ser B) 28:882–887

Podpora C, Lindsley DH (1984) Lindsleyite and mathiasite: synthesis of chromium-titanates in the crichtonite (A1M21O38) series. EOS Trans Am Geophys Union 65:293

Prider RT (1939) Some minerals from the leucite-rich rocks of the west Kimberley area, Western Australia. Min Mag 25:373–387

Rezvukhin DI, Malkovets VG, Sharygin IS, Tretiakova IG, Griffin WL, O'Reilly SY (2018) Inclusions of crichtonite-group minerals in Cr-pyropes from the Internatsionalnaya kimberlite pipe,

Siberian Craton: crystal chemistry, parageneses and relationships to mantle metasomatism. Lithos 308:181–195
Rudnick RL, McDonough WF, O'Connell RJ (1998) Thermal structure, thickness and composition of continental lithosphere. Chem Geol 145:399–415
Safonov OG, Butvina VG (2013) Interaction of model peridotite with H_2O-KCl fluid: experiment at 1.9 GPa and its implications for upper mantle metasomatism. Petrology 21(6):599–615
Safonov OG, Butvina VG (2016) Indicator reactions of K and Na activities in the upper mantle: natural mineral assemblages, experimental data, and thermodynamic modeling. Geochemistry 54(10):858–872
Smyth JR, Erlank AJ, Rickard RS (1978) A new Ba–Sr–Cr–Fe titanate mineral from a kimberlite nodule, vol 59. EOS American Geophysical Union, 394 p
Sobolev NV, Yefimova ES (2000) Composition and petrogenesis of Ti-oxides associated with diamonds. Int Geol Rev 42(8):758–767
Sobolev NV, Yefimova ES, Kaminsky FV, Lavrentiev YG, Usova LV (1988) Titanate of complex composition and phlogopite in the diamond stability field. In: Sobolev NV (ed) Composition and processes of deep seated zones of continental lithosphere. Nauka, Novosibirsk, pp 185–186
Sobolev NV, Yefimova ES, Channer DM DeR, Anderson PFN, Barron KM (1998) Unusual upper mantle beneath Guaniamo, Guyana Shield, Venezuela: evidence from diamond inclusions. Geol 26:971–974
Sokol AG, Kruk AN, Chebotarev DA, Pal'yanov YN, Sobolev NV (2015) Conditions of phlogopite formation upon interaction of carbonate melts with peridotite of the subcratonic lithosphere. Doklady Earth Sci 462(2):638–642
Thibault Y, Edgar AD (1990) Patent mantle-metasomatism: inferences based on experimental studies. Proc Indian Acad Sci-Earth Planet Sci. 99:21–37
Wang L, Essene EJ, Zhang Y (1999) Mineral inclusions in pyrope crystals from Garnet Ridge, Arizona, USA: implications for processes in the upper mantle. Contrib Mineral Pet 135:164–178
Zhang RY, Zhai SM, Fei YW, Liou JG (2003) Titanium solubility in coexisting garnet and clinopyroxene at very high pressure: the significance of exsolved rutile in garnet. Earth Planet Sci Lett 216:591–601
Zhou J (1986) LIL-bearing Ti-Cr-Fe oxides in Chinese kimberlites. In 4th International Kimberlite conference, pp 100–102